Clinical Research in Cardiology (2019) 108:909–920
https://doi.org/10.1007/s00392-019-01421-1

ORIGINAL PAPER

Stress T1-mapping cardiovascular magnetic resonance imaging and inducible myocardial ischemia

Sebastian Bohnen[1] · Lennard Prüßner[1] · E. Vettorazzi[2] · Ulf K. Radunski[1] · Enver Tahir[3] · Jan Schneider[1] · Ersin Cavus[1] · Maxim Avanesov[3] · Christian Stehning[4] · Gerhard Adam[3] · Stefan Blankenberg[1] · Gunnar K. Lund[3] · Kai Muellerleile[1]

Received: 9 September 2018 / Accepted: 24 January 2019 / Published online: 30 January 2019

Abstract

Background Alterations in native myocardial T1 under vasodilation stress ("T1 reactivity") were recently proposed as a non-contrast cardiovascular magnetic resonance (CMR) method to detect myocardial ischemia. This study evaluated the performance of a segmental, truly non-contrast stress T1 mapping CMR approach to detect inducible ischemia.

Methods and results One-hundred patients with suspected/known coronary artery disease underwent CMR at 3.0 or 1.5 T. T1 mapping was performed using the 5s(3s)3s-modified look-locker inversion-recovery (MOLLI) sequence at rest and under regadenoson stress. We defined T1 reactivity as the change in native T1 from rest to stress (1) in the 16-segment AHA model independent from perfusion images and (2) in focal regions of interest that were copied from perfusion images to T1 maps. We compared T1 reactivity between segments/regions with inducible ischemia, scar, and remote myocardium for both approaches. Segmental T1 reactivity was significantly lower in segments including inducible ischemia [−1.15 (95% CI, −2.16 to −0.14)%] compared to remote segments [2.49 (95% CI, 1.87 to 3.11)%; $p<0.001$]. Focal T1 reactivity was also significantly lower [−2.65 (95% CI, −3.84 to −1.46)%] in regions with stress-perfusion defects compared to remote regions [4.72 (95% CI, 3.90 to 5.54)%; $p<0.001$]. However, the performance of segmental T1 reactivity to depict inducible ischemia was significantly inferior compared to the focal approach (AUCs 0.68 versus 0.85; $p<0.0001$).

Conclusions Myocardium with inducible ischemia is characterized by the absence of significant T1 reactivity, but a clinically applicable approach for truly non-contrast stress T1 mapping remains to be determined.

Keywords T1 mapping · T1 reactivity · CMR · Ischemia

Introduction

Non-invasive assessment of myocardial ischemia is a crucial diagnostic step in patients with suspected or known coronary artery disease (CAD) [1–4]. Stress-perfusion-cardiovascular magnetic resonance (CMR) provides important prognostic information [5–7] and is superior compared to single-photon emission computed tomography (SPECT) to detect myocardial ischemia [8–10]. However, stress-perfusion CMR requires the application of gadolinium-based contrast agents, which comes along with the theoretical risks of gadolinium deposition in organs such as the brain after repeated administration [11]. Therefore, non-contrast stress CMR approaches are desirable.

Initial findings by Liu et al. [12] indicate that non-contrast stress T1 mapping could be used to depict myocardium with inducible ischemia. Stress T1-mapping targets changes in

✉ Sebastian Bohnen
s.bohnen@uke.de

1 General and Interventional Cardiology, University Heart Center, University Medical Center Hamburg-Eppendorf, Martinistrasse 52, Hamburg 20246, Germany

2 Department of Medical Biometry and Epidemiology, University Medical Center Hamburg-Eppendorf, Hamburg, Germany

3 Department of Diagnostic and Interventional Radiology and Nuclear Medicine, University Medical Center Hamburg-Eppendorf, Hamburg, Germany

4 Philips Research Hamburg, University Medical Center Hamburg-Eppendorf, Hamburg, Germany

native myocardial T1 during vasodilation stress ("T1 reactivity"), which reflects changes in myocardial blood volume (MBV) related to inducible ischemia [13–16]. T1 reactivity can be measured as focal/ regional differences in native myocardial T1 between vasodilation stress and rest, which was found to be significantly higher in healthy myocardium compared to myocardium with inducible ischemia [12, 17]. However, there is currently a paucity of data on the clinical applicability of stress T1 mapping CMR regarding the performance at different field strengths and different T1-mapping approaches other than the shortened modified look-locker inversion-recovery (shMOLLI) sequence [16, 18]. Thus, we evaluated stress T1 mapping CMR using the 5s(3s)3s-modified look-locker inversion-recovery (MOLLI) sequence to detect inducible ischemia using the standard 16-segment model independent from information of perfusion images in comparison with focal regions of interest that were copied from perfusion images to T1 maps as reference technique.

Methods

Study population and design

This study included 100 consecutive patients with suspected or known CAD, who underwent clinically indicated stress-perfusion CMR for suspected myocardial ischemia. All patients gave their written informed consent and the local ethics committee approved the study. CMR revealed amyloidosis in one patient, tako-tsubo cardiomyopathy in another patient and myocarditis in three patients, who were all excluded from the data analysis. Four patients did not complete CMR due to claustrophobia ($n=2$) or discomfort after stress-perfusion ($n=2$), and these patients were excluded from this analysis due to incomplete data sets. Thus, the final study population consisted of 91 patients who underwent CMR at 3.0 T ($n=42$) or at 1.5 T ($n=49$).

CMR protocol

CMR was performed on a 3.0 T scanner (Ingenia, Philips Medical Systems, Best, The Netherlands) and on a 1.5 T scanner (Achieva, Philips Medical Systems, Best, The Netherlands). The CMR protocol consisted of a standard cine-CMR short-axis stack for the assessment of LV volumes, mass, and function using a standard steady-state free-precession (SSFP) sequence. T1 mapping CMR was performed using a 5s(3s)3s-MOLLI sequence before (= rest) and at 400 µg regadenoson stress (before stress-perfusion CMR) on three representative short-axis slices (basal, midventricular, and apical). Typical imaging parameters of T1 mapping were as follows: voxel size $2\times2\times10$ mm^3, echo time = 0.7 ms, time to repetition = 2.3 ms, partial echo factor = 0.8, flip angle = 35°, SENSE factor = 2, linear phase encoding, ten start-up cycles to approach steady-state prior to imaging, effective inversion times between 134 and 5627 ms. Identical sequence parameter was employed in native T1 mapping at both field strengths, which was chosen to offer a good compromise between T1 accuracy and precision for all T1 in the expected range of 900–1400 ms. T1 mapping was immediately followed by a stress perfusion with an ultrafast gradient echo sequence (balanced Turbo Field Echo (B-TFE) at 1.5 T and T1-weighted TFE (T1TFE) at 3 T) during the first-pass of 0.05 mmol/kg gadoterate meglumine (Dotarem®, Guerbet, Aulnay, France). Finally, phase-sensitive inversion-recovery (PSIR) LGE images on short- and long axes were obtained 10 min after contrast media administration. The CMR protocol with typical imaging parameters and typical acquisition times is presented in Table 1.

General CMR analysis

CMR data were analyzed using the commercially available software cvi42 (Circle Cardiovascular Imaging Inc., Calgary, Alberta, Canada). LV end-diastolic and end-systolic volumes were obtained from cine-CMR short axes to calculate LV stroke volumes (LVSV) as well as LV-ejection fraction (LVEF). LV end-diastolic mass (LVEDM) was obtained including papillary muscles to LVEDM [19]. A clinically relevant definition of inducible myocardial ischemia was used after a consensus reading of stress perfusion and LGE images by two experienced observers in agreement with current recommendations [20]. Inducible ischemia was assumed in myocardium with an inducible stress-perfusion defect that exceeded scar on corresponding LGE images. Myocardial scar was defined as myocardium with LGE, but without an inducible stress-perfusion defect larger than the area of LGE. Remote myocardium was defined by the absence of inducible ischemia and scar. LGE quantification was performed using the 5-SD threshold technique as recommended for ischemic LGE [20].

T1-mapping CMR analysis

Two different approaches for T1-quantification at rest and at stress were used. First, a segmental, blinded approach tested the performance of a truly non-contrast protocol: Endo- and epicardial contours were drawn, manually corrected for motion and carefully aligned with the contours in each respective component image. Rest and stress T1 values were then measured using the recommended 16-segment AHA model [21], independent from any information of corresponding stress-perfusion CMR or LGE images. Second, we performed focal measurements as the reference "proof-of-concept" approach for stress T1-mapping CMR by copying

Table 1 CMR protocol and typical parameters

Modality	Sequence and CMR parameters at 1.5 T	Sequence and CMR parameters at 3.0 T	Typical examination time including planning and pauses
Localizer	B-TFE	TFE	~5 min
	Voxel size: 2.34×4.69×10 mm	Voxel size: 2.34×4.69×10 mm	
	TR: 2.1 ms	TR: 3.8 ms	
	TE: 0.82 ms	TE: 1.82 ms	
	FA: 50°	FA: 20°	
Cine SAX	SSFP	SSFP	~5 min
	Voxel size: 1.98×1.8×8 mm	Voxel size: 2.0×2.0×8 mm	
	TR: 3.1 ms	TR: 2.8	
	TE: 1.57 ms	TE: 1.4	
	FA: 60°	FA: 45°	
Native T1 Mapping at rest	5s(3s)3s-MOLLI	5s(3s)3s-MOLLI	~3 min
	Voxel size: 2.0×2.0×10 mm	Voxel size: 2.0×2.0×10 mm	
	TR: 2.3 ms	TR: 2.3 ms	
	TE: 0.7 ms	TE: 0.7 ms	
	FA: 35°	FA: 35°	
Application of 400 µg regadenoson			~1 min
Native T1 Mapping at stress	5s(3s)3s-MOLLI	5s(3s)3s-MOLLI	~3 min
	Voxel size: 2.0×2.0×10 mm	Voxel size: 2.0×2.0×10 mm	
	TR: 2.3 ms	TR: 2.3 ms	
	TE: 0.7 ms	TE: 0.7 ms	
	FA: 35°	FA: 35°	
First past perfusion during 0.05 mmol/kg gadoterate meglumine	B-TFE	T1TFE	~3 min
	Voxel size: 2.81×2.95×10 mm	Voxel size: 3.0×3.0×10 mm	
	TR: 2.6 ms	TR: 2.4	
	TE: 1.28 ms	TE: 1.1	
	FA: 50°	FA: 20	
Adding up gadoterate meglumine to 0.10 mmol/kg			–
Cine LAX	SSFP	SSFP	~3 min
	Voxel size: 1.99×1.94×8 mm	Voxel size: 2.0×1.6×8 mm	
	TR: 2.8	TR: 2.9 ms	
	TE: 1.4	TE: 1.47 ms	
	FA: 60°	FA: 45°	
Waiting time (10 min after contrast media application)			~7 min
LGE (SAX and LAX)	2D-PSIR	2D-PSIR	~8 min
	Voxel size: 1.6×1.6×8 mm	Voxel size: 1.6×1.9×8 mm	
	TR: 5.3 ms	TR: 6.1	
	TE: 2.6 ms	TE: 3.0	
	FA: 15°	FA: 25°	
Acquisition time of the entire protocol			~35–40 min

B-TFE balanced turbo field echo, *FA* flip angle, *LAX* long-axis view, *LGE* late-gadolinium enhancement, *MOLLI* modified look-locker inversion recovery, *PSIR* phase-sensitive inversion recovery, *SAX* short-axis view, *SSFP* steady-state free precession, *TE* echo time, *TR* repetition time, *T1TFE* T1-weighted TFE

regions of interest from perfusion and LGE images into corresponding T1 maps at rest and at stress in myocardium with inducible ischemia, scar and remote myocardium as defined above. In patients without any inducible ischemia or LGE, standardized measurements of "remote" myocardium were performed in the septum. T1 reactivity was then calculated in % as $\left[\left(n\mathrm{T1}_{\mathrm{stress}} - n\mathrm{T1}_{\mathrm{rest}}\right)/n\mathrm{T1}_{\mathrm{rest}}\right] \times 100$ for both approaches. Figure 1 demonstrates an example for measurements of native T1 at rest and at stress in a patient with inducible myocardial ischemia. Intra- and interobserver

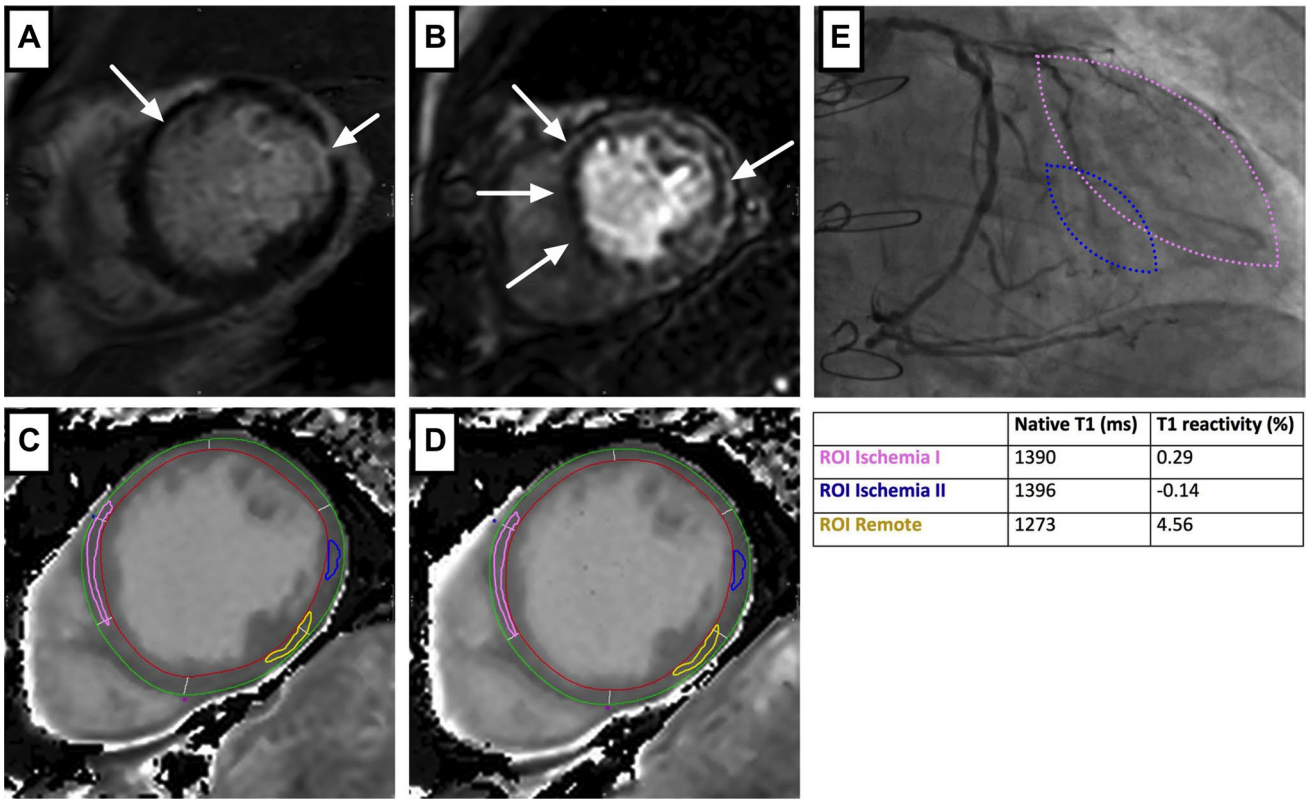

	Native T1 (ms)	T1 reactivity (%)
ROI Ischemia I	1390	0.29
ROI Ischemia II	1396	-0.14
ROI Remote	1273	4.56

Fig. 1 Example CMR measurements at 3.0 T. Late-gadolinium-enhancement (LGE) image **a** demonstrates discreet subendocardial LGE antero-septal and focally transmural LGE of the lateral wall. Stress perfusion **b** shows inducible ischemia exceeding scar antero-septal as well as lateral. **c** Shows the corresponding native rest T1 map and **d** stress T1 map with endo- and epicardial contours for segmental analysis as well as three focal regions of interest (ROI), and **e** demonstrates the coronary angiography of the left coronary artery with an occluded left anterior descending (LAD) and an occluded first marginal branch (M1); furthermore, all venous bypass grafts on two marginal branches and the LAD were occluded (not shown). In both regions with inducible ischemia [ROI Ischemia I (pink) antero-septal and ROI Ischemia II (blue) lateral], rest T1 was elevated and T1 reactivity was 0.29% and −0.14%. In remote myocardium, T1 reactivity was 4.56%

variabilities were obtained by repeated, blinded readings by the same observer and two independent readings by two different, blinded observers, respectively.

Statistical analysis

Statistical analysis was performed using GraphPad Prism version 6.00 (GraphPad Software, San Diego, CA, USA) MedCalc, version 13.3.3.0 (MedCalc Software, Ostend, Belgium) and R version 3.4.2 (R Foundation for Statistical Computing, Vienna, Austria). Descriptive statistics were presented as median and interquartile range (Q_1–Q_3) and compared by Mann–Whitney U test for continuous data, categorical data are presented as numbers and percentage and compared using Fisher's exact test. Intraclass correlation coefficients (ICC) were calculated to assess intra- and interobserver variation. Since segmental and focal measurements of T1 reactivity and native T1 at rest involve repeated measures within the same patient, we used mixed models with a random intercept for the analysis to account for the inherent cluster structure. For segmental data, we used a spatial correlation structure for the within patients error, and a compound symmetry correlation structure was used for focal data. Scanner type (1.5 T and 3 T) and type of myocardium (ischemic, scar, and remote) were entered as fixed effects along with their interaction term. This interaction was removed from the models if it did not improve the model fit using a likelihood ratio test for nested models. Estimated marginal means from the resulting models are reported and compared pairwise. The diagnostic value of T1 reactivity to identify ischemic myocardium was assessed using a Receiver-Operating Characteristics (ROC) analysis. For segmental data, ROC curves were calculated for each segment and were then pooled over all segments. Confidence intervals for the area under the ROC curve (ROC–AUC) and the p value to compare segmental and focal ROC–AUC were calculated using a cluster bootstrap approach with $n = 2000$ replications, where in each replication, a sample of patients from the original population

was drawn with replacement, oppositely to ordinary bootstrap, which samples on observational level. Again, this was done to reflect the hierarchical structure of the data. Two-sided p values were calculated and statistical significance was defined as $p < 0.05$.

Results

General

34 (37%) patients had inducible myocardial ischemia on stress-perfusion CMR and 13 (14%) patients had post-ischemic myocardial scar without inducible myocardial ischemia. Heart rate under regadenoson stress significantly increased from 74 (Q_1–Q_3, 66–89) beats/min to 86 (Q_1–Q_3, 75–100) beats/min ($p = 0.0001$). However, heart rate under regadenoson stress was not significant different between patients with [82 (Q_1–Q_3, 71–100) beats/min] and without inducible ischemia [88 (Q_1–Q_3, 75–103) beats/min, $p = 0.1671$]. More clinical data are presented in Table 2.

T1 reactivity and inducible ischemia—segmental approach

We obtained T1 values in 1456 myocardial segments at rest and after regadenoson stress. However, we had to exclude 255 (17.5%) segments from the data analysis due to artifacts on stress T1 mapping. The intraobserver ICCs of the segmental approach were 0.95 (95% CI, 0.92–0.97) at 3.0 T and 0.94 (95% CI, 0.89–0.97) at 1.5 T. The interobserver ICCs of the segmental approach were 0.91 (95% CI, 0.86–0.95) at 3T and 0.96 (95% CI, 0.92–0.98) at 1.5 T. There were 137 myocardial segments with inducible ischemia (3.0 T $n = 64$ and on 1.5 T $n = 73$) and 81 segments with scar (3.0 T $n = 51$ and 1.5 T $n = 30$). T1 reactivity of myocardial segments including myocardium with inducible ischemia was significantly lower with − 1.15 (95% CI, − 2.16 to − 0.14) % compared to remote myocardial segments with 2.49 (95% CI, 1.87–3.11) %; $p < 0.001$). T1 reactivity of segments including myocardial scar was also lower with 1.13 (95% CI, − 0.07 to 2.33) %, compared to remote myocardial segments ($p = 0.017$) (Table 3; Fig. 2). Segmental T1 reactivity provided an AUC of 0.68 (95% CI, 0.61–0.74) to discriminate between segments with and without inducible ischemia (Fig. 3). The

Table 2 Clinical and CMR parameters

Parameter (unit)	All patients ($n = 91$)	Ischemia ($n = 34$)	No ischemia ($n = 57$)	p value
Age	**59 (51–72)**	**70 (58–76)**	**58 (51–69)**	**0.0045**
Male sex	69/91 (76)	30/34 (88)	41/57 (72)	0.1148
Height (m)	1.77 (1.70–1.80)	1.79 (1.70–1.83)	1.76 (1.69–1.80)	0.1546
Weight (kg)	83 (72–96)	90 (72–98)	80 (66–92)	0.2025
Cholesterol (mg/dl)	152 (133–188)	155 (129–194)	152 (136–182)	0.9919
LDL cholesterol (mg/dl)	76 (56–103)	81 (55–112)	79 (59–103)	0.8707
HDL cholesterol (mg/dl)	46 (40–60)	46 (37–57)	48 (41–65)	0.5258
Creatinine (mg/dl)	0.99 (0.81–1.10)	0.91 (0.82–1.10)	0.99 (0.80–1.10)	0.9687
Creatininkinase (U/l)	110 (65–164)	127 (87–232)	102 (58–156)	0.1618
hs Troponin T (pg/ml)	15 (5–43)	17 (5–49)	15 (5–31)	0.7034
NT-proBNP (pg/ml)	308 (77–919)	471 (74–786)	284 (132–624)	0.9443
Heart rate at rest (bpm)	74 (66–89)	72 (66–89)	74 (67–89)	0.8645
Heart rate at stress (bpm)	86 (74–100)	82 (71–100)	88 (75–103)	0.1671
LVEDVi (ml/m^2)	72 (57–91)	72 (62–105)	71 (55–81)	0.1586
LVESVi (ml/m^2)	20 (12–38)	23 (16–47)	19 (12–27)	0.0650
LVSVi (ml/m^2)	48 (39–57)	46 (39–52)	50 (40–58)	0.4700
LVEDMi (g/m^2)	62 (49–76)	63 (48–85)	58 (49–73)	0.4700
LVEF (%)	**70 (60–78)**	**64 (50–69)**	**75 (66–80)**	**0.0007**
LGE (g)	**0 (0–10)**	**9 (4–17)**	**0 (0–0)**	**< 0.0001**
LGE (%)	**0 (0–6)**	**6 (2–11)**	**0 (0–0)**	**< 0.0001**

Bold–statistical significance was defined as $p < 0.05$

Values are median (first [Q_1] and third [Q_3] quartiles) for continuous and n (% of total column number) for categorical data. p values refer to a comparison between patients with and without inducible ischemia

HDL high density lipoprotein, *LDL* low density lipoprotein, *LGE* late-gadolinium-enhancement, *LVEDVi* left ventricular end-diastolic volume index, *LVESVi* left ventricular end-systolic volume index, *LVSVi* left ventricular stroke volume index, *LVEDMi* left ventricular end-diastolic mass index, *LVEF* left ventricular ejection fraction

Table 3 Segmental, blinded T1 reactivity

Segmental	Inducible ischemia	Scar	Remote	ANOVA *p* value
T1 reactivity (%)	−1.15 (−2.16 to −0.14)[a,b]	1.13 (−0.07 to 2.33)[a]	2.49 (1.87 to 3.11)	**< 0.0001**
3.0 T				
T1 reactivity (%)	−0.55 (−2.11 to 1.00)[a,b]	1.53 (−0.13 to 3.20)	2.60 (1.61 to 3.60)	**< 0.0001**
1.5 T				
T1 reactivity (%)	−2.49 (−3.95 to −1.03)[a,b]	0.55 (−1.38 to 2.48)	2.28 (1.29 to 3.26)	**< 0.0001**

Values are estimated marginal mean (95% CI) for continuous data. Mixed model ANOVA *p* value refers to a comparison between the three different groups

[a]Significant difference between myocardium with inducible ischemia or scar compared to remote myocardium

[b]Significant difference between myocardium with inducible ischemia compared to scar

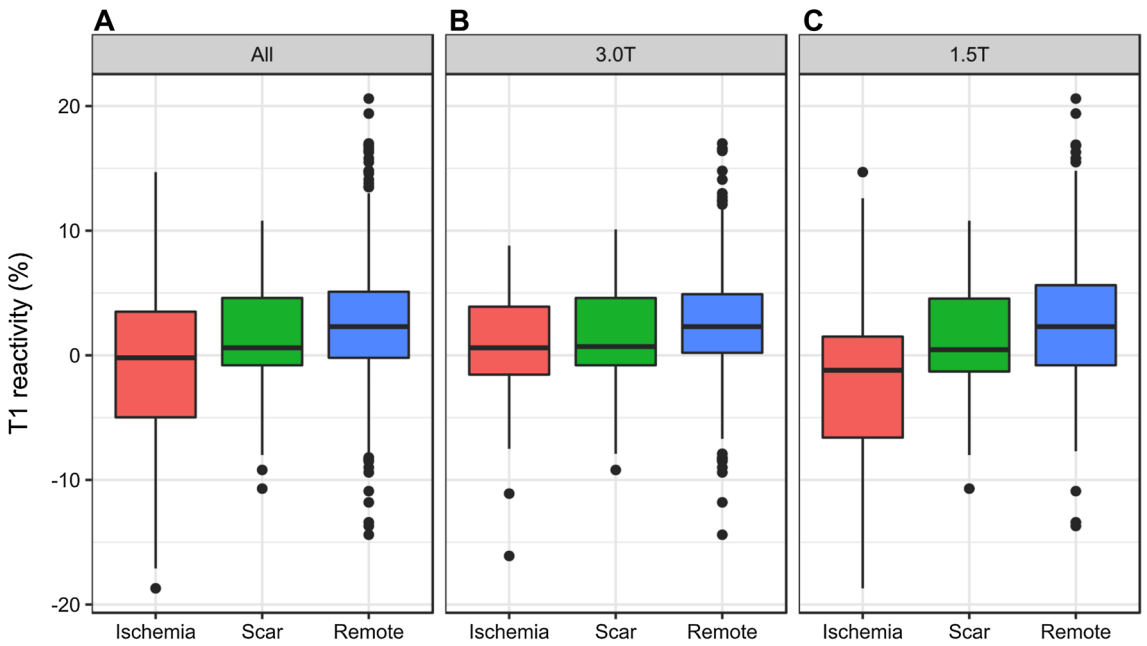

Fig. 2 Segmental T1 reactivity. Segmental T1 reactivity in myocardium with inducible ischemia, scar, and remote myocardium in all patients (**a**), at 3.0 T (**b**), and at 1.5 T (**c**)

optimal cutoff was < 1.55%, which was associated with a sensitivity of 71.0% and specificity of 58.0% to depict inducible myocardial ischemia.

T1 reactivity and inducible ischemia—focal approach

The intraobserver ICCs of the focal approach were 0.92 (95% CI, 0.59–0.98) at 3 T and 0.96 (95% CI, 0.87–0.99) at 1.5 T. The interobserver ICCs of the focal approach were 0.96 (95% CI, 0.79–0.99) at 3 T and 0.95 (95% CI, 0.85–0.98) at 1.5 T. Focal T1 reactivity was significantly lower [− 2.65 (95% CI, − 3.84 to − 1.46)%] in regions with inducible ischemia compared to regions of interest in remote myocardium [4.72 (95% CI, 3.90–5.54)%; $p < 0.001$]. In addition, focal T1 reactivity in regions with scar was significantly lower with − 1.72 [(95% CI, − 3.46 to 0.02)%; $p < 0.001$] compared to remote myocardium (Table 4; Fig. 4). There was no significant difference in T1 reactivity between regions with inducible ischemia and scar. Beyond that, there was no significant difference between findings at 3.0 T and 1.5 T (Table 4; Fig. 4). Focal T1 reactivity provided an AUC of 0.85 (95% CI, 0.78–0.91) to discriminate between myocardium with and without inducible ischemia, which was significantly superior ($p < 0.0001$) compared to the segmental, blinded approach (Fig. 3). The optimal T1 reactivity cutoff was < 1.05% and was associated with a sensitivity of 100% and a specificity of 75.3% to depict inducible myocardial ischemia.

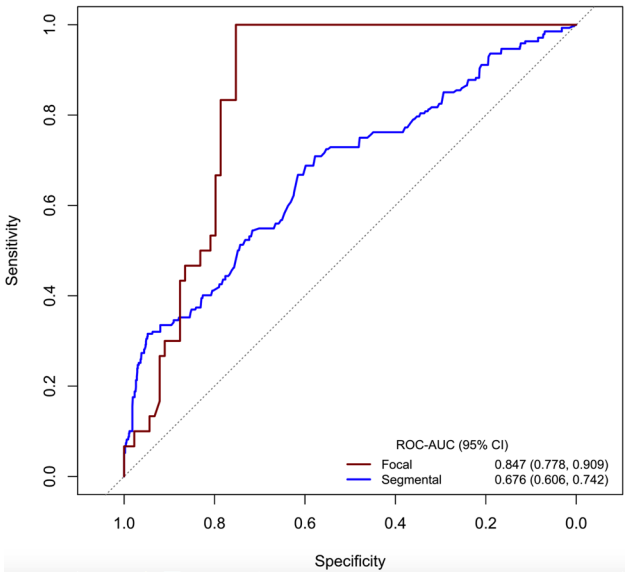

Fig. 3 T1 reactivity for the detection of myocardial ischemia. Receiver operating characteristic (ROC) curves for focal and segmental T1 reactivity to detect myocardial ischemia. Focal T1 reactivity provided a significantly superior area under the curve (AUC) to discriminate between myocardium with inducible myocardial ischemia and remote myocardium compared to the segmental, blinded approach ($p < 0.0001$)

T1 reactivity and inducible ischemia—ischemia only

In the subgroup analysis of patients without any scar on LGE images ($n = 5$ patients with inducible myocardial ischemia, with $n = 22$ myocardial segments with inducible myocardial ischemia), focal T1 reactivity provided an AUC of 0.83 (95% CI, 0.70–0.94) to discriminate between myocardium with and without inducible ischemia, compared to an AUC of 0.75 (95% CI, 0.54–0.89) for the segmental, blinded approach, which was not significantly different ($p = 0.340$).

Native myocardial T1 at rest

Native myocardial T1 at rest was significantly higher in myocardium with inducible ischemia compared to remote myocardium at 3.0 T and 1.5 T (Table 5; Fig. 5). Furthermore, native T1 was significantly elevated in myocardial scar using focal as well as segmental measurements at both field strengths (Table 5; Fig. 5). We did not find significant differences between myocardium with inducible ischemia and scar (Table 5; Fig. 5).

Discussion

We evaluated stress T1-mapping CMR in 91 patients with suspected or known CAD using a 5s(3s)3s MOLLI at 3.0 T and 1.5 T. Our study had three major findings:

- Myocardium with inducible ischemia is characterized by the absence of a significant T1 reactivity under regadenoson stress.
- The performance of a segmental, truly non-contrast T1-reactivity approach to depict inducible ischemia was significantly inferior compared to a focal approach, which requires information from stress perfusion.
- Stress T1 mapping did not enable a reliable differentiation between inducible ischemia and scar.

First, we were able to confirm the general concept of stress T1-mapping CMR by copying regions of interest from stress-perfusion images into rest and stress T1 maps. In agreement with the findings by Liu et al. [12, 18] using shMOLLI and by Kuijpers et al. [17] using 5b(3b)3b MOLLI, we did not find a significant T1 reactivity in myocardium with inducible ischemia using 5s(3s)3s MOLLI. This consistent finding could reflect that myocardial blood volume at rest is already maximally elevated at rest in territories supplied by CA with relevant stenosis and cannot be increased by vasodilation stress [15]. In contrast, myocardial blood volume increases under vasodilation in

Table 4 Focal T1 reactivity

Focal	Inducible ischemia	Scar	Remote	ANOVA p value
T1 reactivity (%)	−2.65 (−3.84 to −1.46)[a]	−1.72 (−3.46 to 0.02)[a]	4.72 (3.90 to 5.54)	**< 0.0001**
3.0 T				
T1 reactivity (%)	−2.39 (−4.21 to −0.58)[a]	−2.29 (−4.91 to 0.34)[a]	4.61 (3.43 to 5.78)	**< 0.0001**
1.5 T				
T1 reactivity (%)	−2.58 (−4.19 to −0.97)[a]	−1.13 (−3.55 to 1.30)[a]	4.83 (3.69 to 5.97)	**< 0.0001**

Values are estimated marginal mean (95% CI) for continuous data. Mixed model ANOVA p value refers to a comparison between the three different groups

[a]Significant difference between myocardium with inducible ischemia or scar compared to remote myocardium

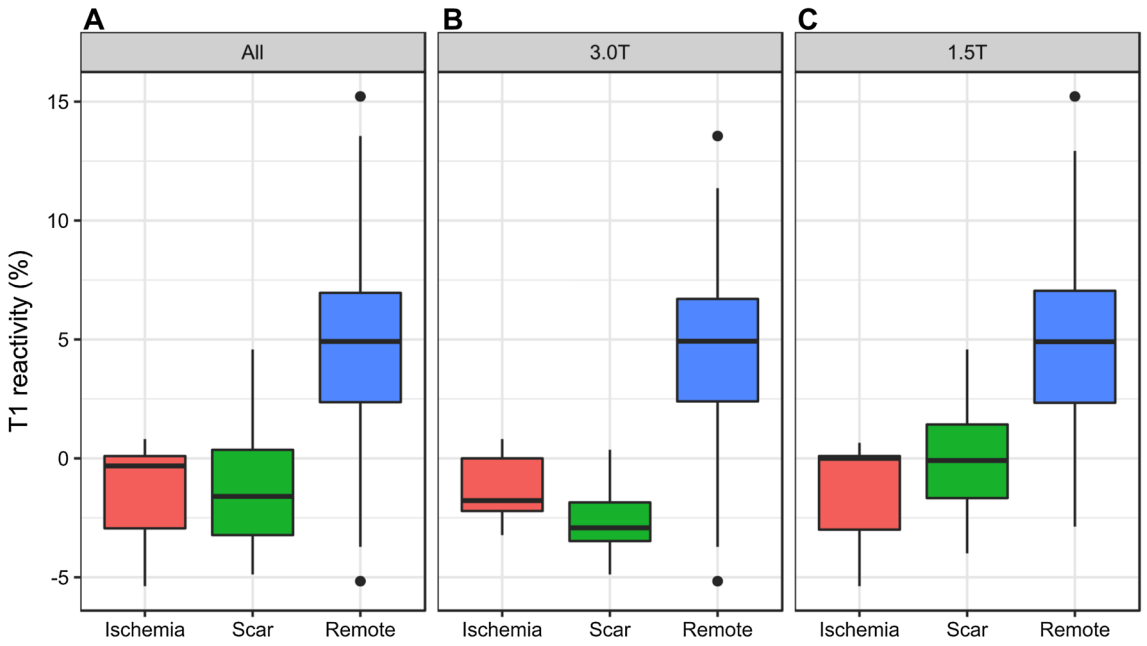

Fig. 4 Focal T1 reactivity. Focal T1 reactivity in myocardium with inducible ischemia, scar, and remote myocardium in all patients (**a**), at 3.0 T (**b**), and at 1.5 T (**c**)

Table 5 Native T1 at rest

Segmental	Inducible ischemia	Scar	Remote	ANOVA *p* value
3.0 T				
Native T1 (ms)	1286 (1267–1306)[a]	1266 (1246–1287)[a]	1235 (1221–1249)	**< 0.0001**
1.5 T				
Native T1 (ms)	1057 (1038–1075)[a]	1049 (1026–1072)[a]	1022 (1008–1035)	**< 0.0001**
Focal				
3.0 T				
Native T1 (ms)	1344 (1311–1377)[a]	1356 (1309–1403)[a]	1225 (1203–1246)	**< 0.0001**
1.5 T				
Native T1 (ms)	1133 (1104–1161)[a]	1128 (1087–1169)[a]	1007 (987–1028)	**< 0.0001**

Values are estimated marginal mean (95% CI) for continuous data. Mixed model ANOVA *p* value refers to a comparison between the three different groups

[a]Significant difference between myocardium with inducible ischemia or scar compared to remote myocardium

healthy myocardium, which is reflected by an increase in native myocardial T1 [12, 17]. The amount of T1 reactivity in remote myocardium [4.72 (95% CI, 3.90–5.54)%] in our study was in line with corresponding values in the works by Liu et al. [12, 18] and by Kuijpers et al. [17]. Thus, our findings clearly substantiate the concept of stress T1 mapping under different conditions, different vendors, T1 mapping sequences, and stress agents. Moreover, our findings highlight that this phenomenon can be observed at 3.0 and 1.5 T. In clinical practice, copying regions of interest from perfusion images to rest/stress T1 maps could be integrated as an additional, confirmative test for equivocal findings in a conventional stress-perfusion protocol. However, this approach does not offer an incremental value in terms of avoiding contrast media and would prolong scan duration.

Thus, we evaluated the potential clinical use of the 16-segment AHA model to detect inducible ischemia by stress T1 mapping. An approach like this would be necessary to provide a truly non-contrast approach. We found that T1 reactivity in myocardial segments with inducible ischemia was significantly lower compared to remote segments at both field strengths. This observation confirms the concept of stress T1 mapping in a blinded segmental approach. However, the performance of this segmental, truly non-contrast

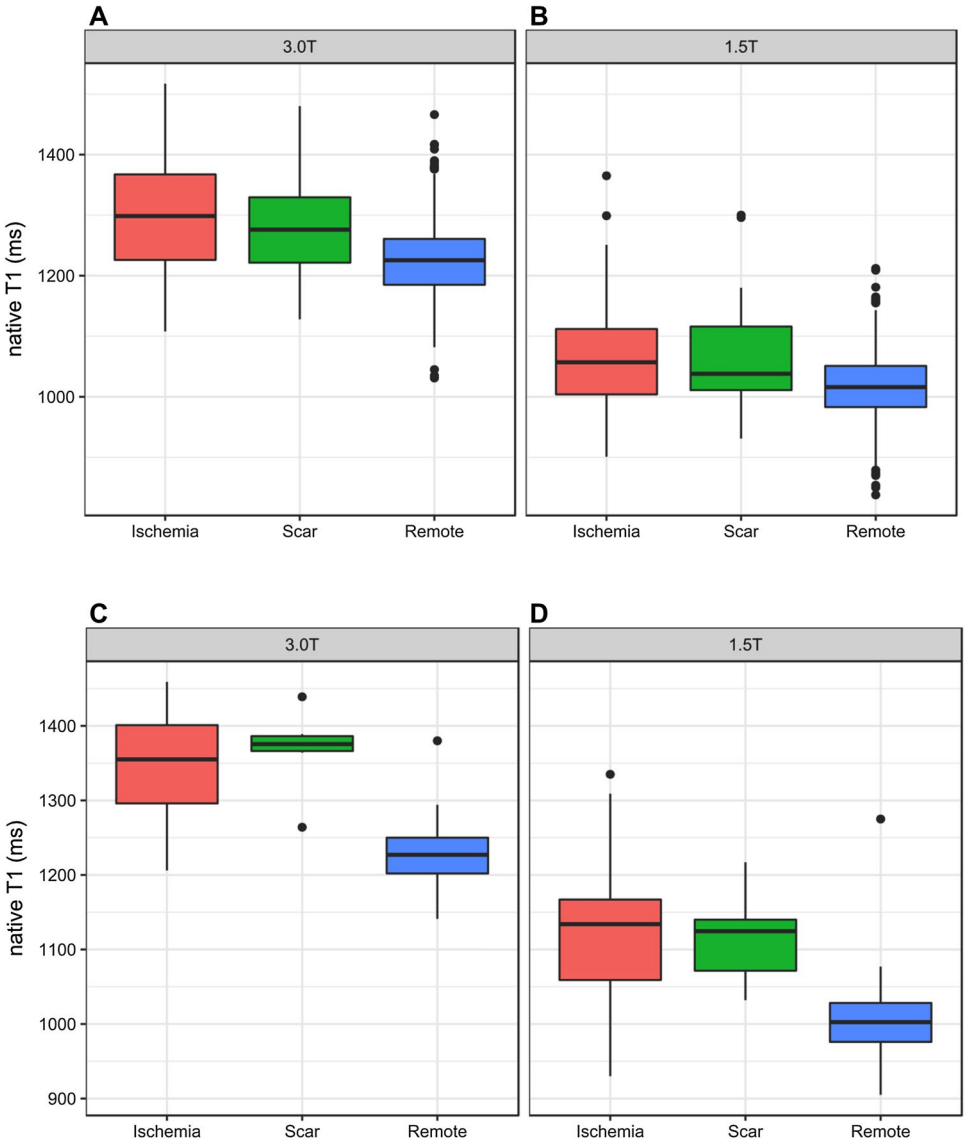

Fig. 5 Native T1 at rest. Native T1 in myocardium with inducible ischemia, scar, and remote myocardium on segmental analysis at 3.0 T (**a**) and at 1.5 T (**b**) and on focal measurements at 3.0 T (**c**) and 1.5 T (**d**)

approach to depict inducible ischemia was significantly inferior compared to the focal approach, which requires information from stress-perfusion images. We think that the inferior performance of this approach compared to the focal approach was related to the coarse spatial resolution of the 16-segment AHA model: Segments of the 16-segment AHA model inevitably contain myocardium with inducible ischemia, scar, and healthy myocardium at the same time and hereby blur tissue-related differences in myocardial T1. On the other hand, this finding could also be related to the use of stress-perfusion CMR as reference technique in our study: Liu et al. recently reported an excellent diagnostic performance for a blinded non-contrast stress T1 mapping approach using FFR as the reference technique [18]. We cannot exclude that the use of FFR as reference technique could have resulted in a different performance of the segmental approach in our study population. In addition, the choice of the T1-mapping sequence could also affect the performance of stress T1 mapping and a head-to-head comparison of the 5s(3s)3s-MOLLI compared to the shMOLLI in stress T1 mapping is still missing [16].

In conclusion, our findings support the general concept of stress T1 mapping, but also clearly showed that the performance of a truly non-contrast segmental approach is currently not sufficient for clinical implementation (Fig. 3). Another important drawback of stress T1 mapping in our study was the high rate (17.51%) of myocardial segments with insufficient image quality under stress.

LGE is currently a valuable part of comprehensive stress-perfusion CMR protocols to detect myocardial scar and to depict non-ischemic diseases. Beyond that, LGE provides crucial prognostic information in ischemic [22, 23] and non-ischemic myocardial disease [24, 25]. In this context, recent studies reported that native T1 is elevated in infarcted

myocardium at 3.0 T and at 1.5 T in patients with acute and chronic myocardial infarction [26–28], but also in other diseases such as myocarditis or amyloidosis [29–33]. Beyond that, native T1 was able to discriminate between acute and chronic myocardial infarction [28] and to differentiate between reversible and irreversible myocardial damage [27]. However, Liu et al. reported only slightly elevated native T1 values at rest in myocardium with inducible ischemia compared to remote myocardium but excessively elevated native T1 values at rest in infarcted myocardium [12, 18]. In the present study, native T1 at rest was elevated in myocardium with inducible ischemia, but also in scar at 3.0 T and at 1.5 T compared to remote myocardium (Table 5). Interestingly, we did not find significant differences between myocardium with inducible ischemia and scar at both field strengths (Table 5; Fig. 5). Thus, our findings seem to contradict the data by Liu et al. [12, 18], which can be explained by a different definition of inducible ischemia: we deliberately included segments/regions with inducible ischemia exceeding subendocardial scar on LGE into our definition of "inducible ischemia", since this definition agrees with current recommendations [20] and seems to be more clinically relevant. However, this inclusion of subendocardial scar may result in "contamination" of native T1 values at rest in segments/regions with inducible ischemia [12, 17]. In conclusion, native T1 at rest is elevated in chronically diseased myocardium at both field strengths without the need of contrast media but a clear differentiation between myocardium with clinically relevant inducible ischemia and pure scar is not possible.

Limitations

One limitation of the present study is the sample size. However, the present study represents a fundament for future studies to evaluate non-contrast approaches by cut-off values established in this cohort. Furthermore, our study does not provide intra-individual comparisons between different field strengths or T1 mapping sequences. Finally, we used stress-perfusion CMR as an accepted non-invasive reference technique for myocardial ischemia, but we did not systematically perform invasive coronary angiography and fractional flow reserve (FFR) for ethical reasons in patients with a negative stress test.

Conclusion

Myocardium with inducible ischemia is characterized by the absence of significant T1 reactivity. The performance of a non-contrast segmental approach is not matured enough for clinical use so far and a clinically applicable approach for truly non-contrast stress T1 mapping remains to be determined.

Funding

This work was supported by the German Heart Foundation/ German Foundation of Heart Research (Grant no. F/21/16).

Compliance with ethical standards

Conflict of interest Dr. Stehning is an employee of Philips Research, Hamburg, Germany. The other authors report no conflicts.

References

1. Rieber J, Huber A, Erhard I, Mueller S, Schweyer M, Koenig A, Schiele TM, Theisen K, Siebert U, Schoenberg SO, Reiser M, Klauss V (2006) Cardiac magnetic resonance perfusion imaging for the functional assessment of coronary artery disease: a comparison with coronary angiography and fractional flow reserve. Eur Heart J 27(12):1465–1471. https://doi.org/10.1093/eurheartj/ehl039
2. Task Force M, Montalescot G, Sechtem U, Achenbach S, Andreotti F, Arden C, Budaj A, Bugiardini R, Crea F, Cuisset T, Di Mario C, Ferreira JR, Gersh BJ, Gitt AK, Hulot JS, Marx N, Opie LH, Pfisterer M, Prescott E, Ruschitzka F, Sabate M, Senior R, Taggart DP, van der Wall EE, Vrints CJ, Guidelines ESCCfP, Zamorano JL, Achenbach S, Baumgartner H, Bax JJ, Bueno H, Dean V, Deaton C, Erol C, Fagard R, Ferrari R, Hasdai D, Hoes AW, Kirchhof P, Knuuti J, Kolh P, Lancellotti P, Linhart A, Nihoyannopoulos P, Piepoli MF, Ponikowski P, Sirnes PA, Tamargo JL, Tendera M, Torbicki A, Wijns W, Windecker S, Document R, Knuuti J, Valgimigli M, Bueno H, Claeys MJ, Donner-Banzhoff N, Erol C, Frank H, Funck-Brentano C, Gaemperli O, Gonzalez-Juanatey JR, Hamilos M, Hasdai D, Husted S, James SK, Kervinen K, Kolh P, Kristensen SD, Lancellotti P, Maggioni AP, Piepoli MF, Pries AR, Romeo F, Ryden L, Simoons ML, Sirnes PA, Steg PG, Timmis A, Wijns W, Windecker S, Yildirir A, Zamorano JL (2013) 2013 ESC guidelines on the management of stable coronary artery disease: the Task Force on the management of stable coronary artery disease of the European Society of Cardiology. Eur Heart J 34(38):2949–3003. https://doi.org/10.1093/eurheartj/eht296
3. Lockie T, Ishida M, Perera D, Chiribiri A, De Silva K, Kozerke S, Marber M, Nagel E, Rezavi R, Redwood S, Plein S (2011) High-resolution magnetic resonance myocardial perfusion imaging at 3.0-Tesla to detect hemodynamically significant coronary stenoses as determined by fractional flow reserve. J Am Coll Cardiol 57(1):70–75. https://doi.org/10.1016/j.jacc.2010.09.019
4. Manka R, Wissmann L, Gebker R, Jogiya R, Motwani M, Frick M, Reinartz S, Schnackenburg B, Niemann M, Gotschy A, Kuhl C, Nagel E, Fleck E, Marx N, Luescher TF, Plein S, Kozerke S (2015) Multicenter evaluation of dynamic three-dimensional magnetic resonance myocardial perfusion imaging for the detection of coronary artery disease defined by fractional flow reserve. Circ Cardiovasc Imaging 8:5. https://doi.org/10.1161/CIRCIMAGING.114.003061
5. Shah R, Heydari B, Coelho-Filho O, Murthy VL, Abbasi S, Feng JH, Pencina M, Neilan TG, Meadows JL, Francis S, Blankstein R, Steigner M, di Carli M, Jerosch-Herold M, Kwong RY (2013)

Stress cardiac magnetic resonance imaging provides effective cardiac risk reclassification in patients with known or suspected stable coronary artery disease. Circulation 128(6):605–614. https://doi.org/10.1161/CIRCULATIONAHA.113.001430
6. Vincenti G, Masci PG, Monney P, Rutz T, Hugelshofer S, Gaxherri M, Muller O, Iglesias JF, Eeckhout E, Lorenzoni V, Pellaton C, Sierro C, Schwitter J (2017) Stress perfusion CMR in patients with known and suspected CAD: prognostic value and optimal ischemic threshold for revascularization. JACC Cardiovasc Imaging 10(5):526–537. https://doi.org/10.1016/j.jcmg.2017.02.006
7. Hendel RC, Friedrich MG, Schulz-Menger J, Zemmrich C, Bengel F, Berman DS, Camici PG, Flamm SD, Le Guludec D, Kim R, Lombardi M, Mahmarian J, Sechtem U, Nagel E (2016) CMR first-pass perfusion for suspected inducible myocardial ischemia. JACC Cardiovasc Imaging 9(11):1338–1348. https://doi.org/10.1016/j.jcmg.2016.09.010
8. Greenwood JP, Maredia N, Younger JF, Brown JM, Nixon J, Everett CC, Bijsterveld P, Ridgway JP, Radjenovic A, Dickinson CJ, Ball SG, Plein S (2012) Cardiovascular magnetic resonance and single-photon emission computed tomography for diagnosis of coronary heart disease (CE-MARC): a prospective trial. Lancet 379(9814):453–460. https://doi.org/10.1016/S0140-6736(11)61335-4
9. Schwitter J, Wacker CM, van Rossum AC, Lombardi M, Al-Saadi N, Ahlstrom H, Dill T, Larsson HB, Flamm SD, Marquardt M, Johansson L (2008) MR-IMPACT: comparison of perfusion-cardiac magnetic resonance with single-photon emission computed tomography for the detection of coronary artery disease in a multicentre, multivendor, randomized trial. Eur Heart J 29(4):480–489. https://doi.org/10.1093/eurheartj/ehm617
10. Schwitter J, Wacker CM, Wilke N, Al-Saadi N, Sauer E, Huettle K, Schonberg SO, Debl K, Strohm O, Ahlstrom H, Dill T, Hoebel N, Simor T, investigators M-I (2012) Superior diagnostic performance of perfusion-cardiovascular magnetic resonance versus SPECT to detect coronary artery disease: the secondary endpoints of the multicenter multivendor MR-IMPACT II (magnetic resonance imaging for myocardial perfusion assessment in coronary artery disease trial). J Cardiovasc Magn Reson 14:61. https://doi.org/10.1186/1532-429X-14-61
11. Gulani V, Calamante F, Shellock FG, Kanal E, Reeder SB, International Society for Magnetic Resonance in M (2017) Gadolinium deposition in the brain: summary of evidence and recommendations. Lancet Neurol 16(7):564–570. https://doi.org/10.1016/S1474-4422(17)30158-8
12. Liu A, Wijesurendra RS, Francis JM, Robson MD, Neubauer S, Piechnik SK, Ferreira VM (2016) Adenosine stress and rest T1 mapping can differentiate between ischemic, infarcted, remote, and normal myocardium without the need for gadolinium contrast agents. JACC Cardiovasc Imaging 9(1):27–36. https://doi.org/10.1016/j.jcmg.2015.08.018
13. Judd RM, Levy BI (1991) Effects of barium-induced cardiac contraction on large- and small-vessel intramyocardial blood volume. Circ Res 68(1):217–225
14. McCommis KS, Zhang H, Goldstein TA, Misselwitz B, Abendschein DR, Gropler RJ, Zheng J (2009) Myocardial blood volume is associated with myocardial oxygen consumption: an experimental study with cardiac magnetic resonance in a canine model. JACC Cardiovasc Imaging 2(11):1313–1320. https://doi.org/10.1016/j.jcmg.2009.07.010
15. Wacker CM, Bauer WR (2003) Myocardial microcirculation in humans—new approaches using MRI. Herz 28(2):74–81. https://doi.org/10.1007/s00059-003-2451-6
16. Piechnik SK, Neubauer S, Ferreira VM (2017) State-of-the-art review: stress T1 mapping-technical considerations, pitfalls and emerging clinical applications. MAGMA. https://doi.org/10.1007/s10334-017-0649-5
17. Kuijpers D, Prakken NH, Vliegenthart R, van Dijkman PR, van der Harst P, Oudkerk M (2016) Caffeine intake inverts the effect of adenosine on myocardial perfusion during stress as measured by T1 mapping. Int J Cardiovasc Imaging 32(10):1545–1553. https://doi.org/10.1007/s10554-016-0949-2
18. Liu A, Wijesurendra RS, Liu JM, Greiser A, Jerosch-Herold M, Forfar JC, Channon KM, Piechnik SK, Neubauer S, Kharbanda RK, Ferreira VM (2018) Gadolinium-free cardiac MR stress T1-mapping to distinguish epicardial from microvascular coronary disease. J Am Coll Cardiol 71(9):957–968. https://doi.org/10.1016/j.jacc.2017.11.071
19. Riffel JH, Schmucker K, Andre F, Ochs M, Hirschberg K, Schaub E, Fritz T, Mueller-Hennessen M, Giannitsis E, Katus HA, Friedrich MG (2018) Cardiovascular magnetic resonance of cardiac morphology and function: impact of different strategies of contour drawing and indexing. Clin Res Cardiol. https://doi.org/10.1007/s00392-018-1371-7
20. Schulz-Menger J, Bluemke DA, Bremerich J, Flamm SD, Fogel MA, Friedrich MG, Kim RJ, von Knobelsdorff-Brenkenhoff F, Kramer CM, Pennell DJ, Plein S, Nagel E (2013) Standardized image interpretation and post processing in cardiovascular magnetic resonance: Society for Cardiovascular Magnetic Resonance (SCMR) board of trustees task force on standardized post processing. J Cardiovasc Magn Reson 15:35. https://doi.org/10.1186/1532-429X-15-35
21. Messroghli DR, Moon JC, Ferreira VM, Grosse-Wortmann L, He T, Kellman P, Mascherbauer J, Nezafat R, Salerno M, Schelbert EB, Taylor AJ, Thompson R, Ugander M, van Heeswijk RB, Friedrich MG (2017) Clinical recommendations for cardiovascular magnetic resonance mapping of T1, T2, T2* and extracellular volume: a consensus statement by the Society for Cardiovascular Magnetic Resonance (SCMR) endorsed by the European Association for Cardiovascular Imaging (EACVI). J Cardiovasc Magn Reson 19(1):75. https://doi.org/10.1186/s12968-017-0389-8
22. Buckert D, Dewes P, Walcher T, Rottbauer W, Bernhardt P (2013) Intermediate-term prognostic value of reversible perfusion deficit diagnosed by adenosine CMR: a prospective follow-up study in a consecutive patient population. JACC Cardiovasc Imaging 6(1):56–63. https://doi.org/10.1016/j.jcmg.2012.08.011
23. Buckert D, Kelle S, Buss S, Korosoglou G, Gebker R, Birkmeyer R, Rottbauer W, Katus H, Pieske B, Bernhardt P (2017) Left ventricular ejection fraction and presence of myocardial necrosis assessed by cardiac magnetic resonance imaging correctly risk stratify patients with stable coronary artery disease: a multi-center all-comers trial. Clin Res Cardiol 106(3):219–229. https://doi.org/10.1007/s00392-016-1042-5
24. Greulich S, Kindermann I, Schumm J, Perne A, Birkmeier S, Grun S, Ong P, Schaufele T, Klingel K, Schneider S, Kandolf R, Bohm M, Sechtem U, Mahrholdt H (2016) Predictors of outcome in patients with parvovirus B19 positive endomyocardial biopsy. Clin Res Cardiol 105(1):37–52. https://doi.org/10.1007/s00392-015-0884-6
25. Grun S, Schumm J, Greulich S, Wagner A, Schneider S, Bruder O, Kispert EM, Hill S, Ong P, Klingel K, Kandolf R, Sechtem U, Mahrholdt H (2012) Long-term follow-up of biopsy-proven viral myocarditis: predictors of mortality and incomplete recovery. J Am Coll Cardiol 59(18):1604–1615. https://doi.org/10.1016/j.jacc.2012.01.007
26. Kali A, Choi EY, Sharif B, Kim YJ, Bi X, Spottiswoode B, Cokic I, Yang HJ, Tighiouart M, Conte AH, Li D, Berman DS, Choi BW, Chang HJ, Dharmakumar R (2015) Native T1 mapping by 3-T CMR imaging for characterization of chronic myocardial infarctions. JACC Cardiovasc Imaging 8(9):1019–1030. https://doi.org/10.1016/j.jcmg.2015.04.018
27. Liu D, Borlotti A, Viliani D, Jerosch-Herold M, Alkhalil M, De Maria GL, Fahrni G, Dawkins S, Wijesurendra R, Francis J,

Ferreira V, Piechnik S, Robson MD, Banning A, Choudhury R, Neubauer S, Channon K, Kharbanda R, Dall'Armellina E (2017) CMR native T1 mapping allows differentiation of reversible versus irreversible myocardial damage in ST-segment-elevation myocardial infarction: an OxAMI study (Oxford acute myocardial infarction). Circ Cardiovasc Imaging 10:8. https://doi.org/10.1161/CIRCIMAGING.116.005986

28. Tahir E, Sinn M, Bohnen S, Avanesov M, Saring D, Stehning C, Schnackenburg B, Eulenburg C, Wien J, Radunski UK, Blankenberg S, Adam G, Higgins CB, Saeed M, Muellerleile K, Lund GK (2017) Acute versus chronic myocardial infarction: diagnostic accuracy of quantitative native T1 and T2 mapping versus assessment of edema on standard T2-weighted cardiovascular MR images for differentiation. Radiology 285(1):83–91. https://doi.org/10.1148/radiol.2017162338
29. Banypersad SM, Fontana M, Maestrini V, Sado DM, Captur G, Petrie A, Piechnik SK, Whelan CJ, Herrey AS, Gillmore JD, Lachmann HJ, Wechalekar AD, Hawkins PN, Moon JC (2015) T1 mapping and survival in systemic light-chain amyloidosis. Eur Heart J 36(4):244–251. https://doi.org/10.1093/eurheartj/ehu444
30. Bietenbeck M, Florian A, Shomanova Z, Klingel K, Yilmaz A (2017) Novel CMR techniques enable detection of even mild autoimmune myocarditis in a patient with systemic lupus erythematosus. Clin Res Cardiol 106(7):560–563. https://doi.org/10.1007/s00392-017-1100-7
31. Bohnen S, Radunski UK, Lund GK, Ojeda F, Looft Y, Senel M, Radziwolek L, Avanesov M, Tahir E, Stehning C, Schnackenburg B, Adam G, Blankenberg S, Muellerleile K (2017) Tissue characterization by T1 and T2 mapping cardiovascular magnetic resonance imaging to monitor myocardial inflammation in healing myocarditis. Eur Heart J Cardiovasc Imaging 18(7):744–751. https://doi.org/10.1093/ehjci/jex007
32. Ferreira VM, Piechnik SK, Dall'Armellina E, Karamitsos TD, Francis JM, Ntusi N, Holloway C, Choudhury RP, Kardos A, Robson MD, Friedrich MG, Neubauer S (2013) T(1) mapping for the diagnosis of acute myocarditis using CMR: comparison to T2-weighted and late gadolinium enhanced imaging. JACC Cardiovasc Imaging 6(10):1048–1058. https://doi.org/10.1016/j.jcmg.2013.03.008
33. Radunski UK, Lund GK, Saring D, Bohnen S, Stehning C, Schnackenburg B, Avanesov M, Tahir E, Adam G, Blankenberg S, Muellerleile K (2017) T1 and T2 mapping cardiovascular magnetic resonance imaging techniques reveal unapparent myocardial injury in patients with myocarditis. Clin Res Cardiol 106(1):10–17. https://doi.org/10.1007/s00392-016-1018-5